

Article

# Parametric Analysis for Hybrid–Electric Regional Aircraft Conceptual Design and Development

Giuseppe Palaia , Karim Abu Salem  and Alessandro A. Quarta \* 

Department of Civil and Industrial Engineering, University of Pisa, Via G. Caruso 8, 56122 Pisa, Italy; giuseppe.palaia@phd.unipi.it (G.P.); karim.abusalem@ing.unipi.it (K.A.S.)

\* Correspondence: alessandro.antonio.quarta@unipi.it

**Abstract:** This paper proposes a conceptual analysis of the limitations related to the development (and integration) of hybrid–electric propulsion on regional transport aircraft, with the aim to identify a feasibility space for this innovative aircraft concept. Hybrid–electric aircraft have attracted the interest of aeronautical research as these have the potential to reduce fuel consumption and, thus, the related greenhouse gas emissions. Nevertheless, considering the development of such an aircraft configuration while keeping the constraints deriving from technological and/or operating aspects loose could lead to the analysis of concepts that are unlikely to be realised. In this paper, specifically to outline the boundaries constraining the actual development of such aircraft, the influence on overall aircraft design and performance of the main technological, operating, and design factors characterising the development of such a configuration is analysed and discussed at a conceptual level. Specifically, the current achievable gravimetric battery energy density (BED) is identified as the main limiting factor for the development of regional hybrid–electric aircraft, and a sensitivity analysis shows the correlation of this important technological parameter with aircraft performance in terms of both fuel consumption and energy efficiency. In this context, minimum technological development thresholds are therefore identified to enable the effective development of this type of aircraft; namely, a minimum of BED = 500 Wh/kg at battery pack level is identified as necessary to provide tangible benefits. From an operating point of view, flight distance is the most limiting design requirement, and a proper assessment of the design range is necessary if a hybrid–electric aircraft is to be designed to achieve lower emissions than the state of the art; flight ranges equal to or lower than 600 nm are to be considered for this type of aircraft. As a bridging of both of the previous constraints, a change in the design paradigm with respect to established practices for state-of-the-art aircraft is necessary. More specifically, penalisations in maximum take-off weight and overall aircraft energy efficiency may be necessary if the aim is to reduce direct in-flight consumption by means of integration of hybrid–electric powertrains.

**Keywords:** hybrid–electric propulsion; battery energy density; aircraft design; regional aviation; aircraft emissions



**Citation:** Palaia, G.; Abu Salem, K.; Quarta, A.A. Parametric Analysis for Hybrid–Electric Regional Aircraft Conceptual Design and Development. *Appl. Sci.* **2023**, *13*, 11113. <https://doi.org/10.3390/app131911113>

Academic Editors: Peter Korba, Miroslav Kelemen and Imre Felde

Received: 29 August 2023

Revised: 29 September 2023

Accepted: 29 September 2023

Published: 9 October 2023



**Copyright:** © 2023 by the authors. Licensee MDPI, Basel, Switzerland. This article is an open access article distributed under the terms and conditions of the Creative Commons Attribution (CC BY) license (<https://creativecommons.org/licenses/by/4.0/>).

## 1. Introduction

A key challenge in the context of aviation research is to find effective solutions to reduce emissions [1–6]. To date, one of the most promising technologies in this regard involves the integration of electric power systems onto transport aircraft [7–12] because electric propulsion can provide high efficiencies and eliminate emissions directly related to the flight. However, there are major technical limitations to the practical application of this technology, arising from the low energy density of batteries even considering the more optimistic forecasts of their technological development, as such important components introduce blocking restrictions in terms of weight and limit the application of electric propulsion to small aircraft only [13]. Currently, more realistically feasible solutions, especially for regional aircraft [14–16], relate to the combination of electric and thermal

propulsion in architectures referred to as hybrid–electric [17–20]. The uncertainty on the actual degree of technological maturity that batteries may reach in the next years makes it tricky to predict what the actual range of use of hybrid–electric aircraft will be in the near future and what return in terms of performance gains can be reasonably achieved.

The aim of this paper is to present a feasibility study and a critical analysis of the performance of a regional hybrid–electric aircraft equipped with parallel powertrain [21–23]. In particular, this work highlights the crucial impact that the level of batteries' technology maturity may have on the expected development of regional hybrid–electric aircraft and analyses their performance, bearing in mind that the main purpose of hybrid–electric aircraft development is to reduce greenhouse emissions. In the latter context, the results may differ (even substantially) from the canonical ones associated with conventional aircraft, which implies the choice of different design strategies. Furthermore, the impact of the proper selection of the design range is widely discussed, highlighting the relevance of the selection of the design requirements together with the operating limitations imposed by the battery weight. The purpose of this paper, therefore, is to illustrate both what the actual design space for future hybrid–electric regional aircraft is, subject to the technological development of electrical energy storage systems, and what is the most appropriate novel design path to develop actual low-emission aircraft.

Specifically, the paper is organized as follows: Section 2 illustrates the design and performance analysis methodology adopted in this work, and Section 3 provides the results and the discussion about the overall aircraft design. In particular, the focus is given to the effect of varying both the battery technology level and the design range. Finally, Section 4 summarizes the conclusions of this research.

## 2. Mathematical Preliminaries and Methodology

The study presented in this paper consists of the design of regional hybrid–electric aircraft and a critical analysis of their performance. In order to identify the context of the study, it is clarified that a regional aircraft is an aeroplane designed primarily to cover short-haul air routes and is usually optimised to serve local and regional communities, connecting cities and airports of limited size. In terms of specifications, regional aircraft usually accommodate between 40 and 80 passengers, with a flight range that typically does not exceed 1000 nautical miles. In general, they are designed to operate on shorter runways than long-haul aircraft, thus requiring greater short take-off and landing capability, and are typically equipped with turboprop engines, which are specifically optimised to reduce costs and fuel consumption on short routes. A comprehensive reference that outlines the regional aviation scenario, also posing a focus on its future development, is proposed in [24], whereas insights on current and advanced regional aircraft and regional airport infrastructures are described in [25–28]. In the proposed research, the top-level aircraft requirements used to steer the design are similar to those of the state-of-the-art benchmark regional aircraft ATR 42, as also proposed in the reference paper [8] and described further along in this section.

The design phase was carried out through the use of the in-house-developed software THEA–CODE, whose detailed description is in [29]. In particular, THEA–CODE performs the multidisciplinary design of a hybrid–electric aircraft, starting from a set of top-level aircraft requirements and taking into account the interdisciplinary links between aerodynamic, structural, propulsive, and aeromechanical features [29]. In this context, the aircraft's aerodynamic polar curve is evaluated by calculating the induced drag using the Vortex Lattice Method [30]; the parasitic drag of the lifting surfaces is calculated by integrating the profile drag coefficient on the wing surface, computed using the XFOIL code; while that of the nacelles, fuselage, and pylons is assessed using the model proposed in [31]. The wing structural mass is calculated using surrogate models based on FEM simulations taking into account the static loading conditions [32], while the structural mass of the fuselage, undercarriage, and tailplane is evaluated by using the models described in [33]. The wing non-structural masses are calculated by means of the method in [34],

while the semi-empirical relationships proposed in [33] are used to evaluate the masses of the on-board systems and operating items. The hybrid–electric propulsion system is sized through the matching chart, which relates aircraft wing loading  $W/S$  to the specific power  $P/W$  necessary for each flight phase [35]. In this context, the required power is allocated in different proportions between electric and thermal chains according to the hybridisation degree  $H_p$ , which is a design variable defined as:

$$H_p = \frac{P_i^e}{P_i^e + P_i^t} \tag{1}$$

where  $P_i^e$  and  $P_i^t$  are the electrical and thermal power installed on-board, respectively.

For each design iteration, a simulation of the mission is carried out by time integration of aircraft equations of motion in the longitudinal plane, as described in detail in [36]. This specific approach gives the amount of fuel and battery mass required to perform the mission, including diversion and reserves, once the power supplied by thermal engines (or electric motor) is assigned. Accordingly, the fraction of power supplied by thermal engines  $\Phi_k^t$  is another design variable, defined as:

$$\Phi_k^t = \frac{P^t}{P_i^t} \tag{2}$$

where  $P^t$  is the power supplied by thermal engine. Note that  $\Phi_k^t$  is assigned for each  $k$ -th mission phase (i.e., climb, cruise, descent, etc.) and allows for the evaluation of also the fraction of electrical supplied power  $\Phi_k^e$ , as the amount of total requested power to fly is known by the mission simulation [36]. The aircraft sizing procedure ends when convergence on the maximum take-off weight (MTOW) is reached. For the present case study, a number of passengers of 40 and a design range of 600 nm, flown at Mach equal to 0.4 and at a height of 6100 m, have been considered as a reference design mission [8]. Specific power values equal to 13 kW/kg, 19 kW/kg, and 352 kWm/kg and efficiency values equal to 0.96, 0.98, and 0.99 have been considered for electric motors, inverters, and wires, respectively [8].

The performance analysis hereafter discussed, having the aim of defining a feasible space in which to develop the regional hybrid–electric aircraft, takes into account the forecasts of battery technology development up to 2035. In this context, a gravimetric battery energy density (BED) sensitivity analysis was carried out to show the current limits of applicability of this technology and highlight the maximum reachable potential. This sensitivity study is conducted by studying the trends of two different figures of merit (FoM): the fuel consumption for the standard mission (i.e., the block fuel  $m_{fb}$ ), and the payload-range efficiency  $PREE$ , defined as:

$$PREE = \frac{m_p g x R}{E} \tag{3}$$

where  $m_p$  is the payload mass;  $g$  is the standard gravity;  $R$  is the range; and  $E$  is the energy, both electrical (stored in the battery) and thermal (stored in the fuel), required to accomplish the mission. Both performance metrics refer to the block mission, i.e., they do not consider the energy and fuel required for diversion and the reserves. The two FoMs,  $PREE$  and block fuel  $m_{fb}$ , were used as objective functions within two different numerical optimisations, set as follows:

$$\left\{ \begin{array}{l} \min(FoM(x)) \\ 0 < H_p < 0.7 \\ 250 < W/S < 325 \\ 0 < \Phi_{cl}^t < 0.56 \\ 0 < \Phi_{cr}^t < 0.56 \\ 0 < \Phi_{de}^t < 0.56 \end{array} \right. \tag{4}$$

The FoM is maximized (or minimised) when it coincides with the *PREE* (or the  $m_{fb}$ ). The design variables selected are  $H_P$ ,  $W/S$ , and  $\Phi_k^t$  for the climb (*cl*), cruise (*cr*), and descent (*de*) of the standard mission; taxiing is accomplished with only electrical power, take-off is performed by supplying total available power, and diversion is conducted with thermal power only to avoid the need of a large amount of unused battery for standard operations. As taxiing and take-off involve the supply of electrical power, the value of  $H_P$  is bound to be larger than zero; hence, the optimiser cannot find full-thermal solutions. The power supply strategy adopted in this work is schematically sketched in Figure 1.

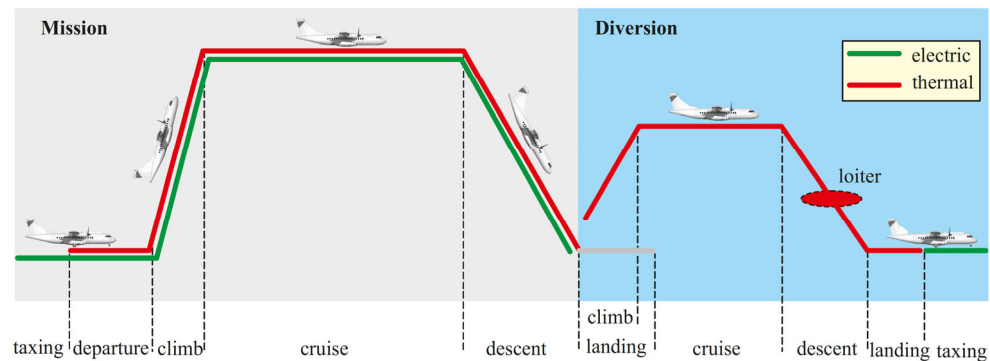


**Figure 1.** Conceptual sketch of hybrid–electric aircraft power supply strategy (adapted from [36]).

The optimisation is performed by coupling a multi-start procedure with local gradient-based algorithms [37].

### 3. Simulation Results and Discussion

This section presents a discussion of the numerical results obtained from the application of the methodology outlined in Section 2. The analysis of the results focuses primarily on the influence of the battery technology level, expressed in terms of *BED*, on the feasibility of regional hybrid–electric aircraft design and their performance. In particular, the performance analysis is critically discussed, highlighting the influence of the selection of different figures of merit on the results. Afterwards, a discussion on the effect of varying the route length on regional hybrid–electric aircraft design is carried out based on the results obtained for ranges smaller than the reference design range, i.e., 400 nm, or larger, i.e., 800 nm, highlighting the significative dependence of the performance of such aircraft configurations on the range value. Overall, this section outlines a general overview, at a conceptual level, of the development potential of regional hybrid–electric aircraft in the next future, depending on the state of the technological development of the main electric components, the requirements for mission range, and the selection of merit figures driving the design.

#### 3.1. Battery Technology Impact on Hybrid–Electric Regional Aircraft Design

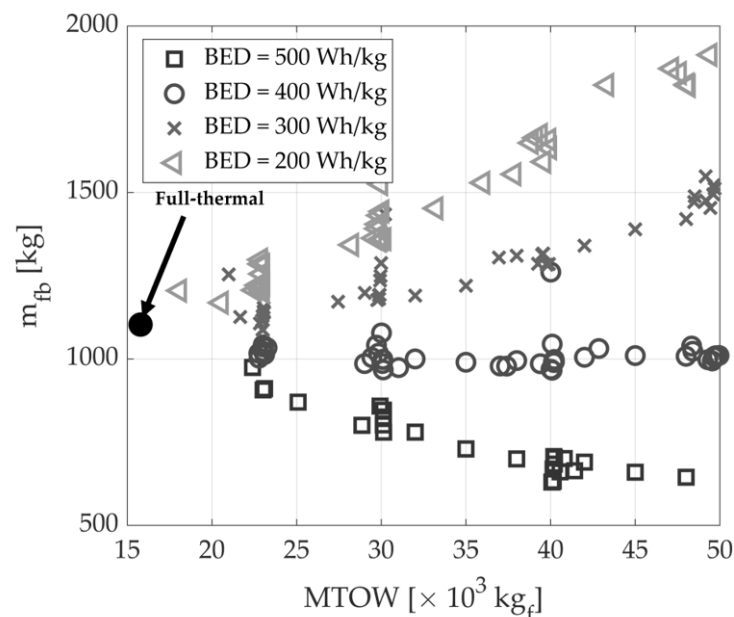
##### 3.1.1. Reference Design Range: 600 nm

The impact of battery technology maturity on overall hybrid–electric aircraft feasibility has been assessed by means of a *BED* sensitivity analysis, varied in the (200, 500) Wh/kg interval [38], considering the complete battery pack. Note that in this range, the lower value is close to the state of the art [39–41], whereas the upper value represents a consolidated forecast for 2035 [42,43]. The reference full–thermal regional aircraft, designed with the same procedure and by enforcing the condition  $H_P = 0$ , exhibits  $MTOW = 15,780$  kg,  $m_{fb} = 1103$  kg, and  $PREE = 0.869$ , while Table 1 shows the data for  $m_{fb}$ -optimised configurations as a function of the *BED* value in the selected range.

**Table 1.** Main data of  $m_{fb}$ -optimised configurations varying  $BED$  @600 nm.

$BED$ (Wh/kg)	$m_{fb}$ (kg)	MTOW (kg <sub>f</sub> )	$H_P$	$W/S$ (kg <sub>f</sub> /m <sup>2</sup> )	$\Phi_{cl}^t$	$\Phi_{cl}^e$	$\Phi_{cr}^t$	$\Phi_{cr}^e$	$\Phi_{de}^t$	$\Phi_{de}^e$
200	1097	17,031	0.139	325	0.548	0.434	0.466	0	0.239	0.412
300	1073	17,462	0.209	325	0.559	0.417	0.471	0	0.172	0.580
400	967	30,116	0.458	325	0.151	0.908	0.433	0.208	0.148	0.220
500	525	50,211	0.459	325	0.088	0.946	0.131	0.524	0.104	0.195

These numerical results highlight two key aspects: (i) Given the state of the art of batteries (but also for incremental technology steps up to 100% with respect to the current achievable value of the  $BED$ ), no significant benefits can be expected from the utilisation of electric power as the weight increases related to the batteries are overwhelming, so the optimal solutions show low in-flight electric power supply; (ii) With an entry-into-service horizon of 2035, the use of hybrid–electric powertrains can contribute to substantial reductions in  $m_{fb}$ , but sharp increases in MTOW must be taken into account. Indeed, for the reference  $BED = 500$  Wh/kg, the advantage in the implementation and utilisation of electrical power, which can be observed from the values of  $H_P$  and  $\Phi_{kr}^e$ , respectively (see Table 1), results in reductions in  $m_{fb}$  but at the expense of a significant increase in MTOW. On the other hand, for lower values of the  $BED$ , the search for power electrification does not introduce a tangible benefit. To better highlight these trends, the optimisations previously described have been carried out by introducing the constraint  $MTOW = W_c$ , with  $W_c$  varied in the  $(15, 50) \times 10^3$  kg<sub>f</sub> interval. In this context, Figure 2 shows the trend of the optimal  $m_{fb}$  obtained as a function of the value of  $W_c$ .

**Figure 2.**  $m_{fb}$  vs. MTOW varying  $BED$ , for optimisations with  $FoM \triangleq m_{fb}$  @600 nm.

From a technical standpoint, increasing the value of  $W_c$  allows for an increase of the amount of the on-board battery power, hence allowing for the growth of the in-flight electrical power utilisation. The simulation results show a worsening trend in terms of  $m_{fb}$  as  $W_c$  increases for values of the  $BED$  equal to 200 and 300 Wh/kg, bringing to light the fact that with these levels of battery technology, the penalties resulting from the weight increases due to the batteries are definitely greater than the benefits of using a share of electrical power to satisfy the energy required for the flight. For a value of the  $BED$  equal to 400 Wh/kg, the beneficial and detrimental effects seem to offset each other, resulting in no noticeable benefit in terms of  $m_{fb}$  as the possible number of batteries on board increases.

The trend is inverted for a *BED* of 500 Wh/kg because the larger the number of batteries on board (hence the possibility of supplying electrical energy in flight), the higher the benefit in terms of  $m_{fb}$  reduction.

In other terms, the level of technological maturity of batteries defines the actual feasibility of regional hybrid–electric aircraft, if benefits in terms of  $m_{fb}$  are the performance index. In fact, as shown in Figure 3, although increasing  $W_c$  allows for similar on-board battery mass increases for all the values of *BED* considered, only the technological value predicted for 2035 provides significant fuel consumption reductions.

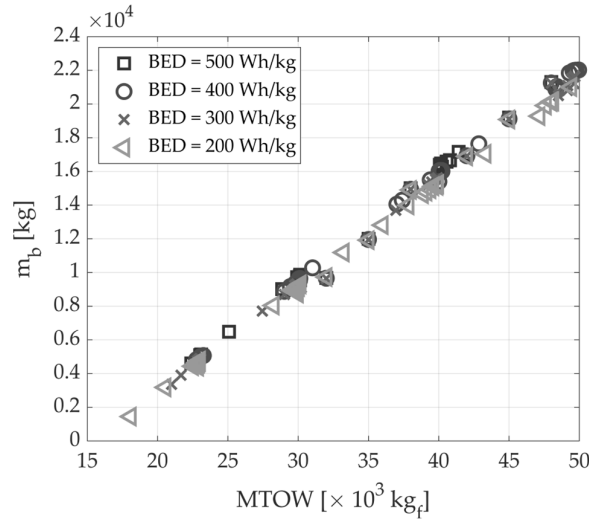


Figure 3.  $m_b$  vs. MTOW varying BED, for optimisations with FoM  $\hat{=} m_{fb}$  @600 nm.

The trend between  $m_{fb}$  and MTOW thus points to an observation regarding the energy efficiency of the hybrid–electric aircraft. In fact, for these optimised configurations, increases in MTOW correspond to reductions in *PREE* for all the *BED* values up to the forecasted reference for the 2035, as shown in Figure 4.

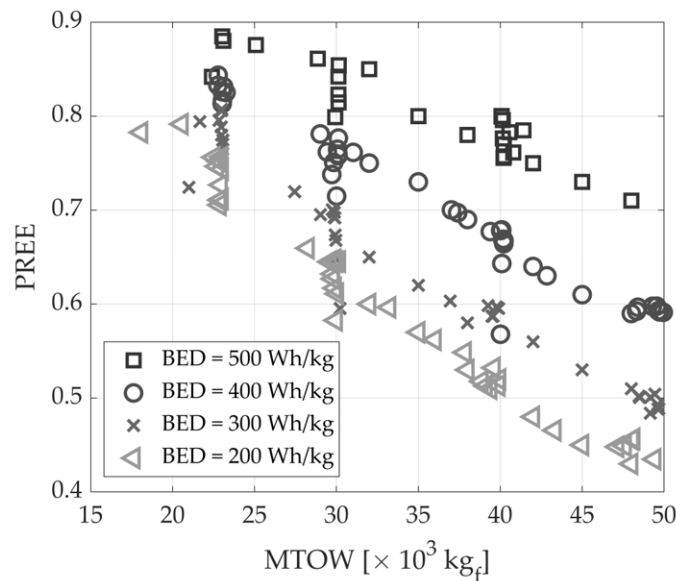


Figure 4. *PREE* vs. MTOW varying BED, for optimisations with FoM  $\hat{=} m_{fb}$  @600 nm.

To discuss this contrast between metrics related to emissions ( $m_{fb}$ ) and those related to aircraft operating efficiency (*PREE*), a second set of optimisations in which the *FoM* to be

maximized was set equal to the *PREE* was performed. In this context, Table 2 shows the obtained results.

**Table 2.** Main data of *PREE*-optimised configurations varying *BED* @600 nm.

<i>BED</i> (Wh/kg)	<i>PREE</i>	MTOW (kg <sub>f</sub> )	<i>H<sub>P</sub></i>	<i>W/S</i> (kg/m <sup>2</sup> )	$\Phi_{cl}^t$	$\Phi_{cl}^e$	$\Phi_{cr}^t$	$\Phi_{cl}^e$	$\Phi_{de}^t$	$\Phi_{de}^e$
200	0.859	16,591	0.084	325	0.501	0.910	0.415	0	0.326	0.061
300	0.882	16,339	0.152	325	0.557	0.415	0.460	0	0.293	0.189
400	0.892	17,393	0.209	325	0.496	0.659	0.473	0	0.175	0.572
500	0.899	21,995	0.403	325	0.294	0.839	0.471	0.173	0.194	0.249

Even for the *PREE*, if we consider the state of the art of the *BED*, the optimal results tend towards configuration with a low in-flight electric power supply, and a similar trend is found for a value of the *BED* equal to 300 Wh/kg. For these configurations, in fact, maximizing the lift-to-drag ratio (hence maximizing the *W/S*) and minimizing the take-off weight coincides with minimizing the energy required for flight *E* and, therefore, since the payload and range are fixed, with maximizing the *PREE*. The situation slightly varies for *BED* = 500 Wh/kg, for which the *PREE*-optimal configuration substantially differs from the *m<sub>fb</sub>*-optimal one. In fact, while exhibiting a non-negligible share of electrical power utilisation, the *PREE* optimum is far from that relevant to *m<sub>fb</sub>* and settles around much lower MTOW values. Once again, it is evident that for hybrid-electric aircraft, conflicts occur that differentiate sizing in the case of seeking solutions oriented towards reducing the fuel consumption (environmental benefits) or increasing the energy-efficiency metrics (operational benefits). To validate this hypothesis, also for the *PREE* optimisations, several runs were performed with the *MTOW* = *W<sub>c</sub>* constraint, whose results are shown in Figure 5. In particular, for a value of the *BED* up to 300 Wh/kg, increasing *W<sub>c</sub>* leads to penalisations in *PREE*, as the main contribution in increasing MTOW results in higher energy required to perform the mission. A slightly different trend is evident for *BED* values equal to 400 and 500 Wh/kg, where the maximum is obtained at *W<sub>c</sub>* larger than the minimum values.

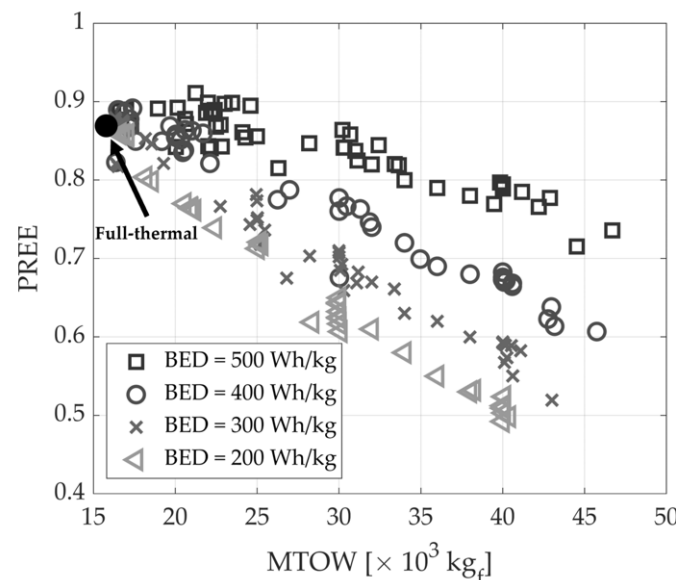


**Figure 5.** *PREE* vs. *MTOW* varying *BED*, for optimisations with FoM  $\triangleq$  *PREE* @600 nm.

This occurs because there is a trade-off between the two different contributions to the energy required for flight because increasing *W<sub>c</sub>* results in a larger energy demand to trim the aircraft in flight, while on the other hand, it allows for an increase in the on-board

battery mass and thus in a higher share of electric power supply. This aspect, for a parallel hybrid–electric powertrain, increases the total propulsive efficiency  $\eta_p$  defined as

$$\eta_p = [(1 - \lambda)\eta_t + \lambda\eta_e]\eta_g \tag{5}$$

where  $\lambda$  is the ratio between the power supplied by the battery and the total supplied power [44]; while  $\eta_t$ ,  $\eta_e$ , and  $\eta_g$  are the efficiencies of the thermal engine, electric motor, and gearbox, respectively. In particular, as discussed in [8], increases in  $\lambda$  (associated with increases in MTOW) imply increments of  $\eta_p$ , as shown in Figure 6 on the left. This propulsive efficiency effect is, however, of minor significance on the overall requested flight energy for a value of the *BED* up to 300 Wh/kg, while it has a beneficial prevalence with respect to the increase in aircraft weight up to 22,000 kg<sub>f</sub> for the case with a value of the *BED* of 500 Wh/kg, where (slight) reductions of *E* can be observed (see the right part of Figure 6).

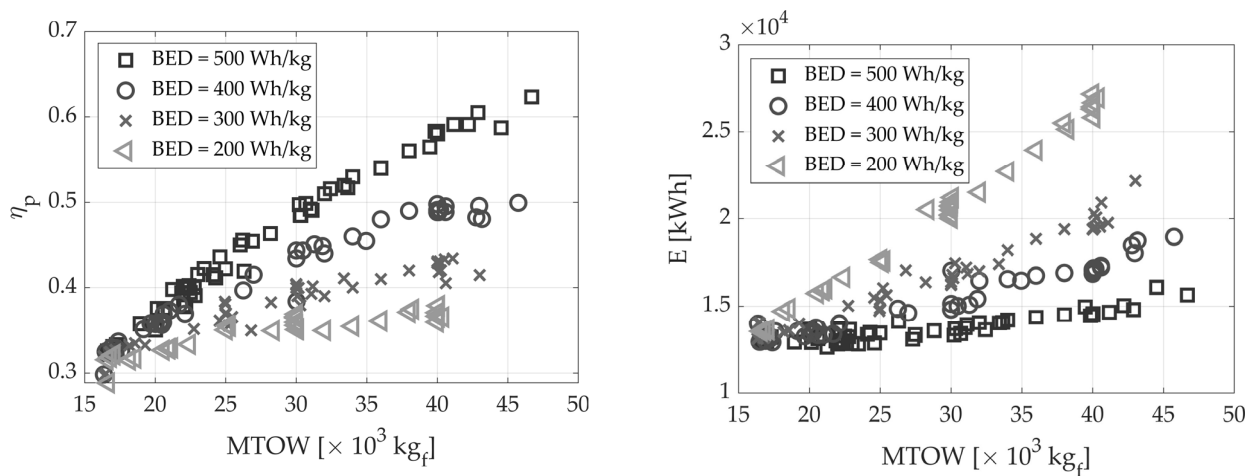


Figure 6. Parallel hybrid–electric powertrain  $\eta$  (left), total energy supplied (right) @600 nm.

Figure 7 shows the results in terms of  $m_{fb}$  for the *PREE*-optimised configurations, in which a similar trend (with respect to MTOW) to that obtained for the  $m_{fb}$ -optimised configurations (see Figure 2) is observed.

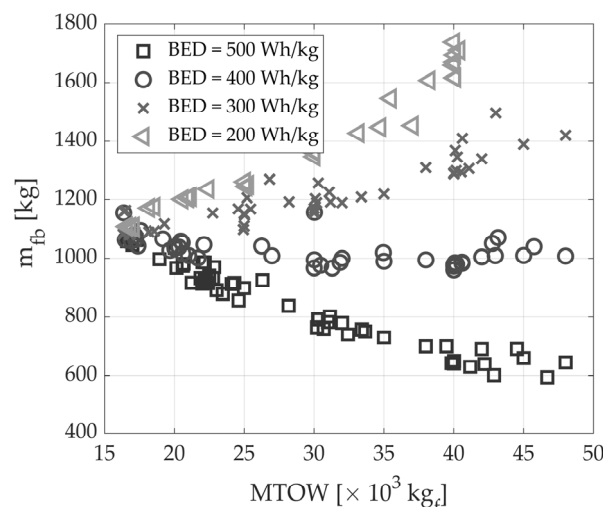


Figure 7.  $m_{fb}$  vs. MTOW varying BED, for optimisations with FoM  $\triangleq$  *PREE* @600 nm.

Setting *PREE* as *FoM*, hence, may lead to a better utilisation of on-board power sources, providing energy-efficient aircraft operations. However, this conduces to solutions that are

close to the thermal-powered aircraft if the current technology for batteries is considered and to a slightly lower-power hybridisation if the technology for 2035 is considered. This aspect does not lead to actual savings in terms of fuel consumption and hence is not an effective strategy to cut greenhouse gas emissions from regional aircraft operations. Indeed, the results here discussed highlight that a paradigm change in conceiving and developing regional hybrid–electric aircraft is necessary to reach the environmental targets for which this technology is under investigation. In fact, with current technology forecasts for 2035, it seems that accepting having a much higher MTOW (and hence energy consumption) than that of the state-of-the-art full-thermal aircraft turns out to be a necessary price to pay if actual emissions benefits are to be achieved. That conclusion is true if we consider only flight-related emissions. Indeed, even in the 2035 technological scenario, the higher energy quota necessary to cut fuel consumption, compatibly replaced by electric energy stored in the batteries, should come from renewable sources if an overall environmental benefit is to be attained.

### 3.1.2. Effect of Varying Design Range

This section describes the effect that design range variations have on the design and performance of regional hybrid–electric aircraft. First, the optimisations described in the previous section were replicated by reducing the design range to 400 nm. That value is representative of many typical missions in the regional market, as documented in [24]. We first present the results for the optimisations in which the  $FoM$  is set equal to the block fuel; then, different sets of optimisations were carried out again to vary the  $MTOW = W_c$  constraint. In Table 3, the results related to the optima– $m_{fb}$  configurations with a design range of 400 nm are reported.

**Table 3.** Main data of  $m_{fb}$ -optimised configurations varying  $BED$  @400 nm.

$BED$ (Wh/kg)	$m_{fb}$ (kg)	MTOW (kg <sub>f</sub> )	$H_P$	$W/S$ (kg/m <sup>2</sup> )	$\Phi_{cl}^t$	$\Phi_{cl}^e$	$\Phi_{cr}^t$	$\Phi_{cl}^e$	$\Phi_{de}^t$	$\Phi_{de}^e$
200	718	18,607	0.136	325	0.456	0.525	0.426	0.367	0.153	0.244
300	525	46,021	0.408	325	0.126	0.482	0.197	0.313	0.160	0.149
400	89	47,204	0.485	325	0.118	0.483	0.01	0.314	0.09	0.148
500	10	37,488	0.694	325	0	0.708	0	0.467	0	0.236

The comparison with the corresponding results obtained for the reference range (namely, 600 nm, see Table 1 and Figure 2) reveals some substantial differences. First, since the energy demand to perform a shorter mission is lower, it is trivial to obtain general reductions in fuel consumption, which is obviously also true for full-thermal configuration. Note that for the full-thermal benchmark,  $MTOW = 15210$  kg<sub>f</sub>,  $m_{fb} = 734$  kg, and  $PREE = 0.871$  are obtained. The differences are thus mainly to be found in the effect of the  $BED$  and  $MTOW$  variations. In fact, it can be observed that as  $MTOW$  increases, even substantial reductions in  $m_{fb}$  can be obtained for  $BED = 400$  Wh/kg (see the left part of Figure 8), a circumstance that did not occur at a range of 600 nm; slight reductions as  $MTOW$  changes are also visible for  $BED = 300$  Wh/kg, which are in any case slight, but considerably better than the results relating to the state of the art in battery technology.

In particular, as  $MTOW$  increases, sharp reductions in  $m_{fb}$  are obtained, both for  $BED$  400 and 500 Wh/kg so that, with respect to the thermal benchmark, reductions of 88% (with an increase in  $MTOW$  of 210%) are obtained for  $BED = 400$  Wh/kg, and even reductions of 97% (with an increase in  $MTOW$  of 146%) are achieved for the  $BED = 500$  Wh/kg case. In this scenario, there is a  $m_{fb} = 10$  kg, i.e., only the take-off share, while the standard airborne mission is fully accomplished with only electrical power. Regarding the values of  $PREE$  obtained for the  $m_{fb}$ -optimised configurations (see the right part of Figure 8), the numerical results show that in case of  $BED = 500$  Wh/kg, the value of the  $PREE$  increases until it reaches a maximum of 1.3 for an  $MTOW$  near 32,000 kg<sub>f</sub>, then the trend is reversed and  $PREE$  decreases. In this case, a more beneficial trade-off between the two

*FoMs* can be selected, as a very low  $m_{fb}$  corresponds with the maximum *PREE*. In the case of  $BED = 400$  Wh/kg, *PREE* is almost constant for the investigated interval of *MTOW*, and for lower values of *BED*, a decreasing trend is still observed, as for the case of 600 nm.

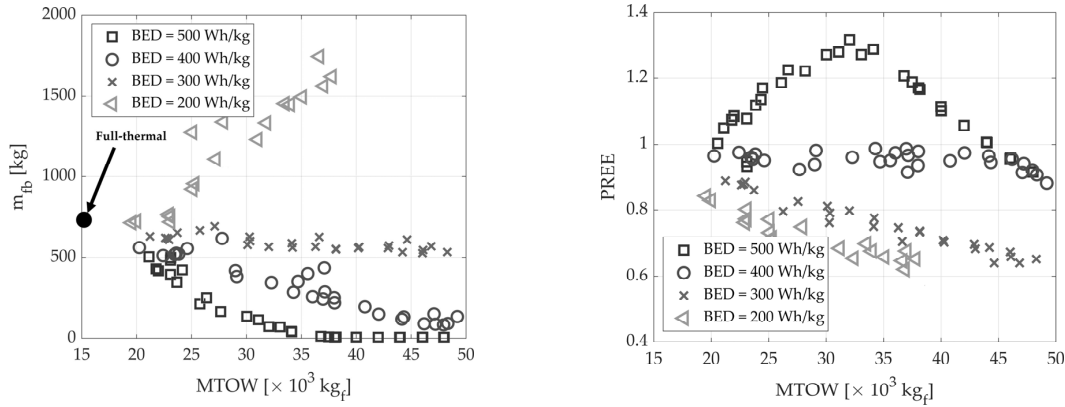


**Figure 8.**  $m_{fb}$  (left), *PREE* vs. *MTOW* (right) varying *BED*; optimisations with  $FoM \hat{=} m_{fb}$ , @400 nm.

Interesting considerations can also be made by evaluating the results for the case where *FoM* is set equal to *PREE* for the 400 nm design range. The results for the *PREE* optima are reported in Table 4, and the trend for the optimisation sets with the constraint  $MTOW = W_c$  is reported in Figure 9. In particular, with respect to the reference case with a design range of 600 nm, in this scenario, increasing the *MTOW* resulted in combined improvements in both the *PREE* and  $m_{fb}$  for  $BED = 500$  Wh/kg; for the *PREE* optimum, a  $m_{fb} = 52$  kg and a *PREE* = 1.335 with a  $MTOW = 32,686$  kg<sub>f</sub> are obtained; the trend of *PREE* with respect to *MTOW* (see the right part of Figure 9) increases up to this maximum, then it starts to rapidly decrease. In the reference case (i.e., 600 nm), on the other hand, increasing the *MTOW* resulted in a very slight, almost imperceptible, peak with a similar trend to that seen for the case at  $BED = 300$  Wh/kg for the reduced range.

**Table 4.** Main data of *PREE*-optimised configurations varying *BED* @400 nm.

<i>BED</i> (Wh/kg)	<i>PREE</i>	<i>MTOW</i> (kg <sub>f</sub> )	$H_P$	$W/S$ (kg/m <sup>2</sup> )	$\Phi_{cl}^t$	$\Phi_{cl}^e$	$\Phi_{cr}^t$	$\Phi_{cl}^e$	$\Phi_{de}^t$	$\Phi_{de}^e$
200	0.889	15,918	0.08	322	0.559	0.406	0.429	0	0.238	0
300	0.908	17,651	0.203	325	0.432	0.913	0.47	0	0.215	0.399
400	1.001	35,102	0.375	325	0.183	1	0.088	0.714	0.163	0.165
500	1.335	32,686	0.421	325	0.126	1	0	1	0.126	0.779

Reducing the range to 400 nm, therefore, would enable an effective implementation of hybrid–electric propulsion with *BED* values reasonably achievable in the next decade. Configurations with potentially low-to-zero fuel consumption in the operating mission can be achieved by considering reduced values for the design range, which in any case would cover the largest share of the regional market [24]. Furthermore, as demonstrated in [36], design range extensions can easily be obtained for hybrid–electric aircraft with parallel powertrain architecture, at the expense of a slight oversizing of the thermal propulsion unit and/or a higher  $m_{fb}$  in these extended-range conditions, considered as off-design routes.

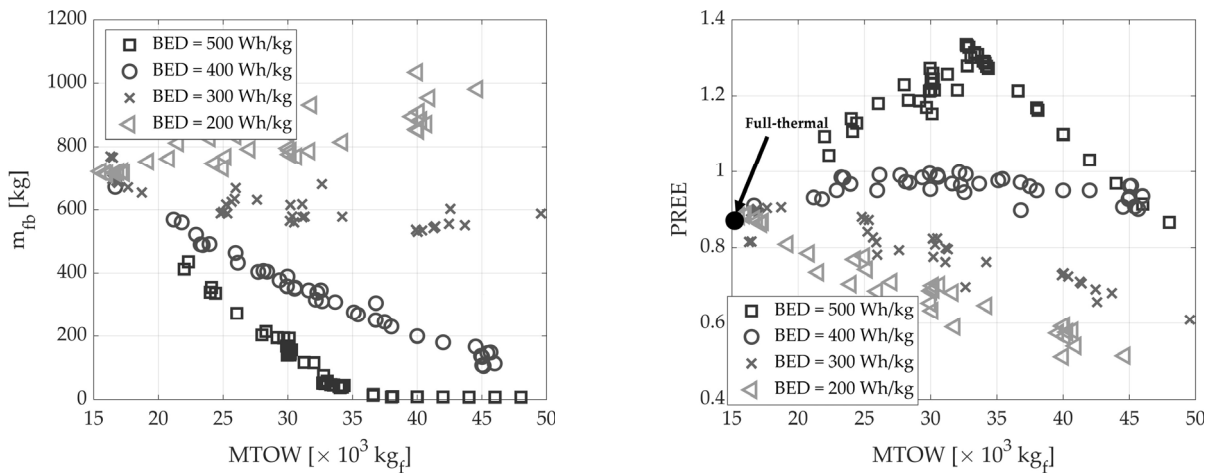


Figure 9.  $m_{fb}$  (left),  $PREE$  vs.  $MTOW$  (right) varying  $BED$ ; optimisations with  $FoM \triangleq PREE @400$  nm.

Increasing the design range with respect to the reference case, on the other hand, leads to opposite observations. This is evident from the trends in Figure 10 and the results in Table 5, obtained by applying the optimisation procedure described in Section 2, using  $FoM$  equal to  $m_{fb}$  for a design range of 800 nm. In addition to the obvious increase in  $m_{fb}$  due to the higher energy demand of the route, there are substantial differences compared to the 600 nm and 400 nm cases. Specifically, increasing the  $MTOW$  does not introduce any significant benefit in terms of  $m_{fb}$  for any  $BED$  value (not even for the most optimistic forecast), as shown in the left part of Figure 10. In fact, the opposite effect is obtained, with deteriorations in fuel consumption for all  $BED$  values except for  $BED = 500$  W/kg, where an almost indifferent trend is obtained. In general, even in this latter case, increasing  $MTOW$  does not bring any benefit, as there is also an associated penalty in terms of the  $PREE$  (see the right part of Figure 10). With respect to the thermal benchmark, which exhibits an  $MTOW = 16,404$  kg<sub>f</sub>, an  $m_{fb} = 1487$  kg, and a  $PREE = 0.859$ , reductions in  $m_{fb}$  of 6.7% (with an increase in  $MTOW$  of 77%) are obtained for  $BED = 500$  Wh/kg, hence not introducing significant overall benefits in this regard, nor are there any benefits in terms of  $PREE$  (see the right part of Figure 10).

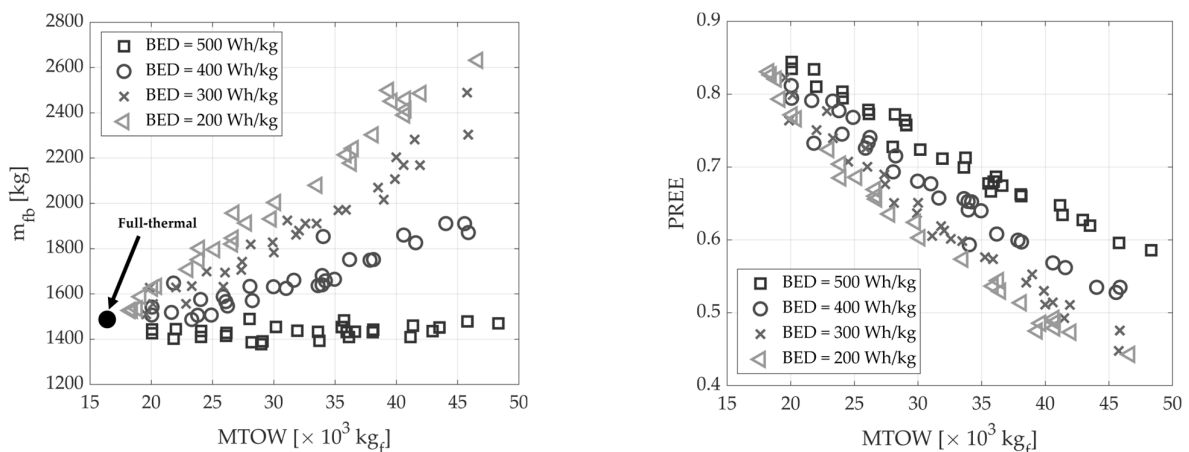


Figure 10.  $m_{fb}$  vs.  $MTOW$  (left),  $PREE$  vs.  $MTOW$  (right) varying  $BED$ , for optimisations with  $FoM \triangleq m_{fb} @800$  nm.

**Table 5.** Main data of  $m_{fb}$ -optimised configurations varying  $BED$  @800 nm.

$BED$ (Wh/kg)	$m_{fb}$ (kg)	MTOW (kg <sub>f</sub> )	$H_P$	W/S (kg/m <sup>2</sup> )	$\Phi_{cl}^t$	$\Phi_{cl}^e$	$\Phi_{cr}^t$	$\Phi_{cl}^e$	$\Phi_{de}^t$	$\Phi_{de}^e$
200	1527	18,277	0.163	325	0.493	0.693	0.438	0	0.291	0.122
300	1509	19,578	0.302	324	0.409	0.794	0.518	0	0.292	0.131
400	1507	20,040	0.338	325	0.520	0.516	0.530	0.015	0.088	0.676
500	1378	28,977	0.337	325	0.242	1	0.349	0.289	0.135	0.282

To summarize, Table 6 reports a concise comparison of the main performance of the  $m_{fb}$ -optimised configurations varying  $BED$  and design range.

**Table 6.** Summary of the comparison of main results for hybrid–electric  $m_{fb}$ -optimised regional configurations, varying  $BED$  and range.

$BED$ (Wh/kg)	MTOW (kg <sub>f</sub> )			$m_{fb}$ (kg)			PREE		
	400 nm	600 nm	800 nm	400 nm	600 nm	800 nm	400 nm	600 nm	800 nm
Full-thermal	15,210	15,783	16,404	734	1103	1487	0.871	0.869	0.859
200	18,607	17,031	18,277	718	1097	1527	0.851	0.862	0.828
300	46,021	17,462	19,578	525	1073	1509	0.675	0.873	0.823
400	47,204	30,116	20,040	89	967	1507	0.941	0.777	0.812
500	37,488	50,211	28,977	10	525	1378	1.188	0.729	0.764

From the previous analyses and discussion, it is apparent that there are three distinct and interdependent boundaries that define a confined field for the effective implementation of hybrid–electric propulsion for regional transport aircraft. The first refers to battery technology development and points out that  $BED$  values (at battery pack level) of 500 Wh/kg must be achieved if effective and efficient integration of hybrid–electric propulsion on transport aircraft is to be envisaged. This is not sufficient unless the aircraft design requirements are properly tuned. In particular, benefits in terms of fuel consumption begin to be achieved if design ranges up to 600 nm are considered. Reducing the range to 400 nm leads to marked improvements in fuel consumption on the standard mission, at the expense of reductions in the aircraft operating capabilities. However, even with these reduced design range values (i.e., 400 nm), most of the typical routes in the current regional sector would be covered. Increasing the design range above 600 nm, on the other hand, would compromise the effectiveness of the integration of hybrid–electric propulsion, as there are no advantages to be gained in terms of fuel consumption and, therefore, no benefit from the reduction of greenhouse gas emissions viewpoint, which is indeed the driver for the development of this technology. The third element required for an effective implementation of hybrid–electric propulsion relates to the selection of figures of merit steering the design process. Specifically, it is highlighted that the technological and weight limitations of batteries need to be overcome through a paradigm shift in design development, in which increases in aircraft weight and reductions in energy efficiency must be taken into account if fuel consumption and related direct greenhouse emissions are to be minimised.

#### 4. Conclusions

The aim of this paper was to identify the feasibility boundaries of regional hybrid–electric aircraft at a conceptual stage. Battery performance, in terms of gravimetric energy density, represents a bottleneck for the effective application of hybrid–electric propulsion in transport aviation. In this paper, a sensitivity analysis in this regard was conducted by considering the design of regional hybrid–electric aircraft equipped with a parallel powertrain. There are two main conclusions that can be summarized from this sensitivity analysis of the results presented in this paper. On the one hand, a clear limitation of the design space is identified, forced by the technological maturity of the batteries, which does

not allow for significant reductions in fuel consumption to be achieved unless the *BED* value of 500 Wh/kg, at pack level, is reached. On the other hand, it emerges that there is a need to change the design paradigm of such aircraft if benefits in terms of reducing greenhouse emissions are to be effectively reached. Specifically, penalties in terms of take-off weight and overall aircraft energy efficiency should be allowed for if real benefits in terms of reducing flight-related emissions are to be achieved. Furthermore, reducing the design range, and hence the operating capability of the regional aircraft, may lead to a substantial reduction in fuel consumption and direct greenhouse gas emissions. That trade-off is crucial and needs to be deeply addressed during the initial phases of the design process of such an innovative aircraft concept.

**Author Contributions:** Conceptualization, K.A.S., G.P. and A.A.Q.; methodology, G.P. and K.A.S.; software, G.P. and K.A.S.; formal analysis, K.A.S. and G.P.; investigation, G.P. and K.A.S.; data curation, G.P. and K.A.S.; writing—original draft preparation, K.A.S. and G.P.; writing—review and editing, A.A.Q.; visualization, G.P. and K.A.S.; supervision, G.P., K.A.S. and A.A.Q. All authors have read and agreed to the published version of the manuscript.

**Funding:** This research received no external funding.

**Institutional Review Board Statement:** Not applicable.

**Informed Consent Statement:** Not applicable.

**Data Availability Statement:** The data presented in this study are available on request from the authors.

**Conflicts of Interest:** The authors declare no conflict of interest.

### Abbreviations

List of Symbols	Description	Unit
$E$	Energy to accomplish the mission	J
$g$	Standard gravity	m/s <sup>2</sup>
$H_p$	Degree of hybridisation	
$L/D$	Lift-to-drag ratio	
$m_b$	Battery mass	kg
$m_{fb}$	Block fuel mass	kg
$m_p$	Payload mass	kg
$P/W$	Specific power	W/kg <sub>f</sub>
$P_i^e$	Electric motor installed power	W
$P_i^t$	Thermal engine installed power	W
$P^t$	Supplied thermal power	W
$R$	Range	nm
$W$	Aircraft weight	N
$W/S$	Wing loading	kg <sub>f</sub> /m <sup>2</sup>
$\eta_e$	Efficiency electric chain	
$\eta_g$	Gearbox efficiency	
$\eta_p$	Propulsion system efficiency	
$\eta_t$	Efficiency thermal chain	
$\lambda$	Source power ratio	
$\Phi^e$	Power fraction supplied by the electric motor	
$\Phi^t$	Power fraction supplied by the thermal engine	
List of acronyms	Description	Unit
BED	Gravimetric battery energy density	Wh/kg
FoM	Figure of merit	
MTOW	Maximum take-off weight	kg <sub>f</sub>
PREE	Payload-range efficiency	

## References

1. Lee, D.; Pitari, G.; Grewe, V.; Gierens, K.; Penner, J.; Petzold, A.; Prather, M.; Schumann, U.; Bais, A.; Berntsen, T.; et al. Transport impacts on atmosphere and climate: Aviation. *Atmospheric Environ.* **2010**, *44*, 4678–4734. [[CrossRef](#)] [[PubMed](#)]
2. Hudda, N.; Durant, L.W.; Fruin, S.A.; Durant, J.L. Impacts of Aviation Emissions on Near-Airport Residential Air Quality. *Environ. Sci. Technol.* **2020**, *54*, 8580–8588. [[CrossRef](#)] [[PubMed](#)]
3. Hasan, A.; Al Mamun, A.; Rahman, S.M.; Malik, K.; Al Amran, I.U.; Khondaker, A.N.; Reshi, O.; Tiwari, S.P.; Alismail, F.S. Climate Change Mitigation Pathways for the Aviation Sector. *Sustainability* **2021**, *13*, 3656. [[CrossRef](#)]
4. Tasca, A.L.; Cipolla, V.; Abu Salem, K.; Puccini, M. Innovative Box-Wing Aircraft: Emissions and Climate Change. *Sustainability* **2021**, *13*, 3282. [[CrossRef](#)]
5. Ciliberti, D.; Della Vecchia, P.; Memmolo, V.; Nicolosi, F.; Wortmann, G.; Ricci, F. The Enabling Technologies for a Quasi-Zero Emissions Commuter Aircraft. *Aerospace* **2022**, *9*, 319. [[CrossRef](#)]
6. Proesmans, P.-J.; Vos, R. Airplane Design Optimization for Minimal Global Warming Impact. *J. Aircr.* **2022**, *59*, 1363–1381. [[CrossRef](#)]
7. Brelje, B.J.; Martins, J.R. Electric, hybrid, and turboelectric fixed-wing aircraft: A review of concepts, models, and design approaches. *Prog. Aerosp. Sci.* **2018**, *104*, 1–19. [[CrossRef](#)]
8. Abu Salem, K.; Palaia, G.; Quarta, A.A. Review of hybrid-electric aircraft technologies and designs: Critical analysis and novel solutions. *Prog. Aerosp. Sci.* **2023**, *141*, 100924. [[CrossRef](#)]
9. Zhang, X.; Bowman, C.L.; O’Connell, T.C.; Haran, K.S. Large electric machines for aircraft electric propulsion. *IET Electr. Power Appl.* **2018**, *12*, 767–779. [[CrossRef](#)]
10. Sahoo, S.; Zhao, X.; Kyprianidis, K. A Review of Concepts, Benefits, and Challenges for Future Electrical Propulsion-Based Aircraft. *Aerospace* **2020**, *7*, 44. [[CrossRef](#)]
11. Barzkar, A.; Ghassemi, M. Electric Power Systems in More and All Electric Aircraft: A Review. *IEEE Access* **2020**, *8*, 169314–169332. [[CrossRef](#)]
12. Wheeler, P.; Sirimanna, T.S.; Bozhko, S.; Haran, K.S. Electric/Hybrid-Electric Aircraft Propulsion Systems. *Proc. IEEE* **2021**, *109*, 1115–1127. [[CrossRef](#)]
13. Abu Salem, K.; Palaia, G.; Quarta, A.A.; Chiarelli, M.R. Medium-Range Aircraft Conceptual Design from a Local Air Quality and Climate Change Viewpoint. *Energies* **2023**, *16*, 4013. [[CrossRef](#)]
14. Voskuil, M.; van Bogaert, J.; Rao, A.G. Analysis and design of hybrid electric regional turboprop aircraft. *CEAS Aeronaut. J.* **2018**, *9*, 15–25. [[CrossRef](#)]
15. Eisenhut, D.; Windels, E.; Reis, R.; Bergmann, D.; Ilário, C.; Palazzo, F.; Strohmayer, A. Foundations towards the future: FutPrInt50 TLARs an open approach. *IOP Conf. Series Mater. Sci. Eng.* **2021**, *1024*, 012069. [[CrossRef](#)]
16. Brdnik, A.P.; Kamnik, R.; Marksel, M.; Božičnik, S. Market and Technological Perspectives for the New Generation of Regional Passenger Aircraft. *Energies* **2019**, *12*, 1864. [[CrossRef](#)]
17. Friedrich, C.; Robertson, P. Hybrid-Electric Propulsion for Aircraft. *J. Aircr.* **2015**, *52*, 176–189. [[CrossRef](#)]
18. Hoelzen, J.; Liu, Y.; Bensmann, B.; Winnefeld, C.; Elham, A.; Friedrichs, J.; Hanke-Rauschenbach, R. Conceptual Design of Operation Strategies for Hybrid Electric Aircraft. *Energies* **2018**, *11*, 217. [[CrossRef](#)]
19. Pornet, C.; Isikveren, A. Conceptual design of hybrid-electric transport aircraft. *Prog. Aerosp. Sci.* **2015**, *79*, 114–135. [[CrossRef](#)]
20. Sgueglia, A.; Schmollgruber, P.; Bartoli, N.; Benard, E.; Morlier, J.; Jasa, J.; Martins, J.R.R.A.; Hwang, J.T.; Gray, J.S. Multidisciplinary Design Optimization Framework with Coupled Derivative Computation for Hybrid Aircraft. *J. Aircr.* **2020**, *57*, 715–729. [[CrossRef](#)]
21. Finger, D.F.; Braun, C.; Bil, C. Comparative assessment of parallel-hybrid-electric propulsion systems for four different aircraft. *J. Aircr.* **2020**, *57*. [[CrossRef](#)]
22. Decerio, D.P.; Hall, D.K. Benefits of Parallel Hybrid Electric Propulsion for Transport Aircraft. *IEEE Trans. Transp. Electrification* **2022**, *8*, 4054–4066. [[CrossRef](#)]
23. De Vries, R.; Brown, M.; Vos, R. Preliminary Sizing Method for Hybrid-Electric Distributed-Propulsion Aircraft. *J. Aircr.* **2019**, *56*, 2172–2188. [[CrossRef](#)]
24. Eisenhut, D.; Moebs, N.; Windels, E.; Bergmann, D.; Geiß, I.; Reis, R.; Strohmayer, A. Aircraft Requirements for Sustainable Regional Aviation. *Aerospace* **2021**, *8*, 61. [[CrossRef](#)]
25. Della Vecchia, P.; Nicolosi, F. Aerodynamic guidelines in the design and optimization of new regional turboprop aircraft. *Aerosp. Sci. Technol.* **2014**, *38*, 88–104. [[CrossRef](#)]
26. Nicolosi, F.; Corcione, S.; Trifari, V.; De Marco, A. Design and Optimization of a Large Turboprop Aircraft. *Aerospace* **2021**, *8*, 132. [[CrossRef](#)]
27. Palaia, G.; Abu Salem, K.; Quarta, A.A. Comparative Analysis of Hybrid-Electric Regional Aircraft with Tube-and-Wing and Box-Wing Airframes: A Performance Study. *Appl. Sci.* **2023**, *13*, 7894. [[CrossRef](#)]
28. Meindl, M.; de Ruiter, C.; Marciello, V.; Di Stasio, M.; Hilpert, F.; Ruocco, M.; Nicolosi, F.; Thonemann, N.; Saavedra-Rubio, K.; Locqueville, L.; et al. Decarbonised Future Regional Airport Infrastructure. *Aerospace* **2023**, *10*, 283. [[CrossRef](#)]
29. Palaia, G.; Zanetti, D.; Abu Salem, K.; Cipolla, V.; Binante, V. THEA-CODE: A design tool for the conceptual design of hybrid-electric aircraft with conventional or unconventional airframe configurations. *Mech. Ind.* **2021**, *22*, 19. [[CrossRef](#)]

30. Drela, M.; Youngren, H. *AVL 3.36 User Primer, 3.36*; Online Software Manual; Massachusetts Institute of Technology: Massachusetts, CA, USA, 2017; Available online: [https://web.mit.edu/drela/Public/web/avl/AVL\\_User\\_Primer.pdf](https://web.mit.edu/drela/Public/web/avl/AVL_User_Primer.pdf) (accessed on 28 August 2023).
31. Raymer, P. *Aircraft Design: A Conceptual Approach*; AIAA Education Series; American Institute of Aeronautics & Ast.: Washington, DC, USA, 1992; ISBN 0-930403-51-7.
32. Cipolla, V.; Abu Salem, K.; Palaia, G.; Binante, V.; Zanetti, D. A DoE-based approach for the implementation of structural surrogate models in the early stage design of box-wing aircraft. *Aerosp. Sci. Technol.* **2021**, *117*, 106968. [[CrossRef](#)]
33. Wells, D.; Horvath, B.; McCullers, L. *The Flight Optimization System Weights Estimation Method*; NASA Technical Report; NASA: Washington, DC, USA, 2017. Available online: <https://ntrs.nasa.gov/citations/20170005851> (accessed on 28 August 2023).
34. Torenbeek, E. *Development and Application of a Comprehensive, Design Sensitive Weight Prediction Method for Wing Structures of Transport Category Aircraft*; Report LR-693; Delft University of Technology: Delft, The Netherlands, 1992.
35. Sforza, P. *Commercial Airplane Design Principles*; Elsevier: Amsterdam, The Netherlands, 2014. [[CrossRef](#)]
36. Palaia, G.; Abu Salem, K. Mission Performance Analysis of Hybrid-Electric Regional Aircraft. *Aerospace* **2023**, *10*, 246. [[CrossRef](#)]
37. Martins, J.R.; Ning, A. *Engineering Design Optimization*; Cambridge University Press: Cambridge, UK, 2021; ISBN 978-1108833417.
38. Zhao, L.; Lakraychi, A.E.; Chen, Z.; Liang, Y.; Yao, Y. Roadmap of Solid-State Lithium-Organic Batteries toward 500 Wh kg<sup>-1</sup>. *ACS Energy Lett.* **2021**, *6*, 3287–3306. [[CrossRef](#)]
39. Marciello, V.; Di Stasio, M.; Ruocco, M.; Trifari, V.; Nicolosi, F.; Meindl, M.; Lemoine, B.; Caliandro, P. Design Exploration for Sustainable Regional Hybrid-Electric Aircraft: A Study Based on Technology Forecasts. *Aerospace* **2023**, *10*, 165. [[CrossRef](#)]
40. L bberding, H.; Wessel, S.; Offermanns, C.; Kehrer, M.; Rother, J.; Heimes, H.; Kampker, A. From Cell to Battery System in BEVs: Analysis of System Packing Efficiency and Cell Types. *World Electr. Veh. J.* **2020**, *11*, 77. [[CrossRef](#)]
41. Xue, N.; Du, W.; Martins, J.R.R.A.; Shyy, W. Lithium-Ion Batteries: Thermomechanics, Performance, and Design Optimization. In *Handbook of Clean Energy Systems*; Encyclopedia of Aircraft Engineering, Green Aviation; John Wiley & Sons, Ltd.: Hoboken, NJ, USA, 2015; pp. 1–16. [[CrossRef](#)]
42. Dever, T.; Duffy, K.; Provenza, A.J.; Loyselle, P.L.; Choi, B.B.; Morrison, C.R.; Lowe, A.M. *Assessment of Technologies for Noncryogenic Hybrid Electric Propulsion*; Report NASA, TP-2015-216588; NASA: Washington, DC, USA, 2015. Available online: <https://ntrs.nasa.gov/citations/20150000747> (accessed on 28 August 2023).
43. Zhang, H.; Li, X.; Zhang, H. *Li-S and Li-O<sub>2</sub> Batteries with High Specific Energy*; Springer: Singapore, 2017; pp. 1–48. [[CrossRef](#)]
44. Isikveren, A.; Kaiser, S.; Pernet, C.; Vratny, P. Pre-design strategies and sizing techniques for dual-energy aircraft. *Aircr. Eng. Aerosp. Technol.* **2014**, *86*, 525–542. [[CrossRef](#)]

**Disclaimer/Publisher’s Note:** The statements, opinions and data contained in all publications are solely those of the individual author(s) and contributor(s) and not of MDPI and/or the editor(s). MDPI and/or the editor(s) disclaim responsibility for any injury to people or property resulting from any ideas, methods, instructions or products referred to in the content.